

1  
2  
3  
4  
5  
6  
7

# COMPARING SHORT-TERM SEISMIC AND COVID-19 FATALITY RISKS IN ITALY

Eugenio Chioccarelli,<sup>a</sup> Iunio Iervolino<sup>b</sup>

<sup>a</sup> *Dipartimento di Ingegneria Civile, dell'Energia, dell'Ambiente e dei Materiali, Università degli studi Mediterranea di Reggio Calabria, Reggio Calabria, Italy, [eugenio.chioccarelli@unirc.it](mailto:eugenio.chioccarelli@unirc.it).*

<sup>b</sup> *Dipartimento di Strutture per l'Ingegneria e l'Architettura, Università degli Studi di Napoli Federico II, via Claudio 21, 80125, Naples, Italy, [iunio.iervolino@unina.it](mailto:iunio.iervolino@unina.it). **Corresponding author***

8 **ABSTRACT**

9 Risks assessment and risks comparison are basic concepts for emergency management. In the fields of  
10 earthquake engineering and engineering seismology, the operational earthquake loss forecasting (OELF)  
11 is the research frontier for the assessment of short-term seismic risk. It combines seismicity models,  
12 continuously updated based on ground motion monitoring (i.e., operational earthquake forecasting), with  
13 large-scale vulnerability models for the built environment and exposure data. With the aim of contributing  
14 to the discussion about capabilities and limitations of OELF, the study presented aimed at comparing the  
15 OELF results and the fatality risk related to CoVid-19 that, at the time of writing, is perceived as very  
16 relevant and required unprecedented risk reduction measures in several countries, most notably Italy.  
17 Results show that, at a national scale in Italy, the CoVid-19 risk has been higher than the seismic risk during  
18 the two pandemic waves, even if, at the end of the so-called lockdown, the evolution of the pandemic  
19 suggested the possibility (not realized) of reaching a situation of comparable seismic and CoVid-19 risks  
20 in a few weeks. Because the two risks vary at a local scale, risks comparison was also carried out on a  
21 regional basis, showing that, before the beginning of the second wave, in some cases, the seismic risk, as  
22 assessed by means of OELF, was larger than the pandemic one.

23 **Keywords:** Operational earthquake loss forecasting, SARS-Cov-2 pandemic, lockdown, emergency  
24 management.

## 25 INTRODUCTION

26 Due to the work of the *Istituto Nazionale di Geofisica e Vulcanologia* or INGV, Italy is provided with a  
27 system for operational earthquake forecasting (OEF), now named *OEF-Italy* (Marzocchi *et al.*, 2014),  
28 which, based on the seismic activity recorded via the national monitoring network, is used to  
29 probabilistically forecast the weekly expected number of earthquakes in the whole country. On this basis,  
30 the *Rete Nazionale dei Laboratori di Ingegneria Sismica* (ReLUIS) developed a system, named MANTIS-K  
31 (Iervolino *et al.*, 2015) that, based on the OEF data, produces *operational earthquake loss forecasting*  
32 (OELF) information. MANTIS-K combines the weekly seismicity rates, with vulnerability and inventory  
33 models for the Italian building stock, so as to obtain weekly forecasts of seismic risk (consequences)  
34 metrics, that is: the expected number of damaged buildings, injured citizens, and fatalities. OEF and OELF  
35 are the edge of research in the earthquake engineering and engineering seismology fields and have been  
36 the object of a scientific debate on their usefulness, communicability and understandability (e.g., Wang  
37 and Rogers, 2014). In order to contribute to the discussion, in this study the outputs of MANTIS-K are  
38 compared with the threat from the *severe acute respiratory syndrome coronavirus 2* or SARS-Cov-2, or  
39 CoVid-19 hereafter, that is an interesting term of comparison for reasons that will be clarified in the  
40 following.

41 In Italy, the first two cases of CoVid-19 were detected in two Chinese tourists on January 30<sup>th</sup>, 2020, one  
42 day before that the *World Health Organization* declared the international emergency. The first case of  
43 autochthonous contagion in Italy was confirmed on February 18<sup>th</sup> and the first death for CoVid-19 was  
44 recorded on the 24<sup>th</sup> of the same month. Then, in accordance with data provided the *Italian Civil*  
45 *Protection Department* (see Data and Resources), the daily number of fatalities attributed to CoVid-19 in  
46 Italy rapidly increased and a national lockdown was declared starting from March 9<sup>th</sup>, which was partially  
47 relieved on May 18<sup>th</sup>. The maximum number of deaths per day was reached on March 27<sup>th</sup> and it is equal  
48 to 969. After that day, a period of constant decrease of deaths (i.e., the end of the first wave) has been

49 recorded until the beginning of August when the number of deaths started increasing again i.e., a second  
50 wave started. The maximum (daily) number of deaths during the second wave was higher than the first  
51 one: 993 deaths were recorded on December 3<sup>rd</sup>. Despite that, mainly for economic reasons, another  
52 national lockdown was not declared, while differentiated regional measures to control the pandemic were  
53 enforced and weekly adapted to the pandemic evolution. At the time of writing, the total number of  
54 observed fatalities in Italy attributed to CoVid-19 (in most of cases they are related to people with other  
55 pathologies as well; see Data and Resources) is 69214 (last updated, 21<sup>st</sup> of December 2020).

56 In order to compare the risks related to earthquakes and CoVid-19, MANTIS-K forecasts in terms of  
57 expected number of fatalities are divided by the population in the country, from census data, to obtain  
58 the earthquake fatality rates. On the other hand, because consolidated forecasting models for deaths due  
59 to CoVid-19 are not available (at least to the authors), the observed weekly fatality rates due to the  
60 infection are adopted as a representative metric of the risk; they can be interpreted as the weekly  
61 probability that a citizen in Italy, selected randomly, is found dead because of CoVid-19 (being derived by  
62 the data provided by the Italian Civil Protection Department, uncertainties on these data are assumed to  
63 be negligible). Both seismic and CoVid-19 fatality rates are discussed at both national and local (regional)  
64 scale. Moreover, a risk comparison is also provided assuming the scenario of a seismic sequence similar  
65 to the one of L'Aquila 2009 (mainshock moment magnitude,  $M_w$ , equal to 6.1), which killed about three-  
66 hundred people.

67 Before proceeding any further, it must be noted that seismic and CoVid-19 related risks are, in general,  
68 not stochastically independent because, for example, a major seismic sequence can interfere with the  
69 strategies (i.e., lockdown or social distancing) to control the evolution of the pandemic (Peng, 2020).  
70 However, recent works suggest that the pandemic did not significantly affected the response capacity of  
71 official authorities to seismic events (Pankow *et al.*, 2020; Margheriti *et al.*, 2021). In the following, the

72 two risks are treated independently as their interaction is outside of the purposes of the study, if not  
73 distracting for its conclusions.

74 In the remaining part of the paper, the framework and the models adopted for OELF are described first.  
75 Then seismic and CoVid-19 fatality risks are compared at both national and regional scale. Subsequently,  
76 the main implications that can be drawn from the results are discussed. A section of conclusions ends the  
77 paper.

## 78 **OPERATIONAL EARTHQUAKE LOSS FORECASTING**

79 The loss forecasting model is grounded on the fact that, given a region monitored by a seismic sensor  
80 network (Gorini *et al.*, 2010), OEF provides, for each cell in which the territory is divided and identified by  
81 the coordinates  $\{x, y\}$ , the expected number, per week, of earthquakes above a certain magnitude. Such  
82 a rate (density),  $\lambda$ , depends on the recent (recorded) seismic history,  $H(t)$ , and then varies with time.  
83 Indeed, it is computed combining three models of earthquake forecasting: two of them are alternative  
84 versions of the epidemic-type aftershocks sequences (ETAS; see Marzocchi *et al.*, 2014 for details) and the  
85 third is the short-term earthquakes probabilities (STEP) model proposed by Woessner *et al.* (2010). The  
86 cell characterized by the  $\{x, y\}$  coordinates can be treated as a point-like seismic source. In the OEF-Italy  
87 system, the magnitude distribution of these events is assumed to be of the Gutenberg-Richter-type  
88 (Gutenberg and Richter, 1944), with unlimited maximum magnitude and  $b$ -value equal to one (all point  
89 sources share the same magnitude distribution.)

90 Considering now a site, identified by  $\{w, z\}$  coordinates, with distance  $R$  from  $\{x, y\}$ , in which there is  
91 exposure to seismic risk, for example buildings and their residents, it is possible to use the rate above as  
92 an input to get the rate of events causing some casualty or consequence of interest,  $\lambda_{Cas^{(k)}}$ . Indeed,  
93 assuming that the building belongs to a category ( $k$ ) for which a vulnerability model is available, the

94 casualty rate is given in equation (1), where the integral over  $x$  and  $y$  variables accounts for the fact that  
 95 the  $\{w, z\}$  site may be subject to several point sources.

$$\begin{aligned}
 \lambda_{Cas^{(k)}}(t, w, z | H(t)) &= \iint_{x,y} \lambda(t, x, y | H(t)) \cdot \sum_{ds} P[Cas^{(k)} | ds] \cdot \\
 &\cdot \sum_{ms} P[DS^{(k)} = ds | ms] \cdot \int_m P[MS = ms | m, R] \cdot f_M(m) \cdot dm \cdot dx \cdot dy
 \end{aligned}
 \tag{1}$$

97 In the equation:  $f_M(m)$  is the mentioned distribution of magnitude,  $M$ , for one event occurring at a  
 98 source cell;  $P[MS = ms | m, R]$  is the probability of one event hits the  $\{w, z\}$  site showing seismic intensity  
 99  $MS$  equal to  $ms$ , given magnitude and source-to site distance, that is from a seismic intensity prediction  
 100 equation;  $P[DS^{(k)} = ds | ms]$  is the probability that  $ms$  intensity causes damage state  $DS$  equal to  $ds$   
 101 for the building of the structural typology under consideration, that is a probabilistic measure of the  
 102 vulnerability of the building of interest; and  $P[Cas^{(k)} | ds]$  is the probability that such casualty (e.g.,  
 103 injuries or fatalities) occurs to a resident of the building of that structural typology in the case the building  
 104 suffers  $ds$  damage state.

105 In the short-term, for example for one week, it is legitimated to consider the rate of events causing some  
 106 casualty is constant. If number of buildings of each structural typology,  $N_P^{(k)}$ , is known for the  $\{w, z\}$   
 107 site, and if the time interval  $(t, t + \Delta t)$  is small, then the expected number of casualties can be computed  
 108 via equation (2). Such a result represents the *expected number of casualties* in the  $\Delta t$  at the site  $\{w, z\}$

109 following the OEF rates release,  $E[N_{Cas,(t,t+\Delta t,w,z)} | H(t)]:$

$$E[N_{Cas,(t,t+\Delta t,w,z)} | H(t)] \approx \sum_k N_P^{(k)} \cdot \lambda_{Cas^{(k)}}(t, w, z | H(t)) \cdot \Delta t
 \tag{2}$$

111 The expected total number of causalities in a region or in the whole country can be computed summing  
 112 up the results of equation (2) over the considered sites.

113 The OELF procedure set up is compliant with the performance-based earthquake engineering framework  
114 where the decision variable for risk management is the probabilistic loss, which is a function, via the total  
115 probability theorem, of hazard, vulnerability, and exposure (Cornell and Krawinkler, 2000). The adopted  
116 models for the OELF system in Italy are described in the following section.

## 117 **MODEL COMPONENTS**

118 In MANTIS-K the hazard is represented by the OEF rates and by the seismic intensity (probabilistic)  
119 prediction model. The weekly earthquake rates, with magnitude equal or larger than four, from the OEF-  
120 Italy system, are provided as an input of the OELF procedure for a grid of seismic sources spaced of about  
121 0.1° and covering the whole national territory and some surroundings, which are relevant for risk  
122 assessment. They are obtained from the seismicity recorded by a country-wide seismic network and are  
123 updated daily or every three hours after an earthquake with magnitude equal or larger than 3.5. The  
124 seismic intensity prediction model considered (Pasolini *et al.*, 2008) is specific for Italy and refers to the  
125 Mercalli-Cancani-Sieberg (MCS) scale (Sieberg, 1931).

126 The vulnerability model is made of the ensemble of damage probabilities for each possible MCS intensity,  
127 that is a damage probability matrix or DPM and from the probability of casualties given damage state of  
128 a building of a certain typology. The system has embedded DPM that are based on post-event damage  
129 recognitions (Zuccaro and Cacace, 2009) in recent earthquakes in Italy and are those employed, by the  
130 Italian Civil Protection, for seismic scenario analyses. The considered DPM features four vulnerability  
131 categories covering the majority of structural typologies for residential buildings in Italy. Damage states  
132 considered by the DPM are six: *no damage*, *slight damage*, *moderate damage*, *heavy damage*, *very heavy*  
133 *damage*, *collapse*. Vulnerability classes, damage levels and macroseismic scale, to which the DPM refers,  
134 are defined in accordance with the European macroseismic scale or EMS 98 (Grünthal, 1998). Casualty

135 (injuries or fatalities) probabilities conditional to a given structural damage,  $P[Cas^{(k)}|ds]$ , are also a  
136 library of the system and are taken from the work of Zuccaro and Cacace (2011).  
137 To account for exposure, municipalities are the elementary units in which the Italian territory is divided.  
138 The number of buildings and the number of residents (both grouped by vulnerability class) are derived  
139 from the Italian census of 2001 and are embedded in the OELF system. According to the casualty model  
140 considered (Zuccaro *et al.*, 2012), risk assessment may be carried out considering that 65% of the total  
141 population is exposed at the time of occurrence of the earthquake, that is, the term  $N_p^{(k)}$  is multiplied  
142 by 0.65 in equation (2). A more refined occupancy versus-time distribution based on empirical data is  
143 virtually allowed by the OELF model.  
144 Thus, as described in more details by Iervolino *et al.* (2015), MANTIS-K provides risk assessment with a  
145 probabilistically-consistent approach and, in addition to the uncertainties in earthquake occurrence and  
146 magnitude considered by the OEF models it has as an input, it accounts for uncertainties in: (i) ground  
147 motion intensity produced by an earthquake of given magnitude and location; (ii) observed damage in a  
148 building of a given typology, given the ground motion intensity at the construction site; (iii) consequences  
149 due to a specific structural damage; (iv) residents exposed to structural failure at the time of the  
150 earthquake. On the other hand, MANTIS-K has some limitations related to the non-evolutionary  
151 characteristics of the vulnerability and exposure models (Chioccarelli and Iervolino, 2016); however,  
152 studies to overcome such limitations are underway (Iervolino *et al.*, 2020).

## 153 **RISKS COMPARISON**

154 In this section, all discussed results are in terms of weekly death rates, that is, number of fatalities per  
155 week divided by the population available from the *Istituto Nazionale di Statistica* or ISTAT (see the Data  
156 and Resources section). This is to allow comparisons between different geographical scales. Indeed, the



157 national scale is first considered. Then, comparisons of risks at smaller, regional, scales are discussed. This  
158 is because both the CoVid-19 and earthquake risks vary significantly across Italy.

### 159 **NATIONAL SCALE**

160 The black line of Figure 1 shows the weekly forecasted rates of deaths in Italy due to earthquakes (*EQ*  
161 *Fatality* in the legend) estimated by the OELF system from the 2<sup>nd</sup> of February to the 6<sup>th</sup> of December,  
162 2020 thus in a period that includes the national lockdown in Italy (starting and ending date of the  
163 lockdown are represented in the figure by the grey vertical lines), when the whole population was basically  
164 required to stay home continuously. As shown, the rates are almost constant, equal to about  $7E-08$ ,  
165 because no major seismic sequences occurred in Italy in the considered interval (i.e., it represents the  
166 background seismic fatality risk in Italy). Thus, assuming that the national forecasted seismicity does not  
167 significantly change in the subsequent weeks, the estimated death rates are extrapolated as shown by the  
168 dotted black line.

169 The red curve of Figure 1, identified as *C19 Fatality* in the legend, shows, for each Sunday, the weekly  
170 rates of observed fatalities in Italy due to CoVid-19 infection and are available until the end of December  
171 (i.e., at time of writing). Data shows that after a rapid increase, since the beginning of April the rates  
172 started decreasing until the beginning of August when a new increasing period started, reaching a new  
173 (local) maximum in December 2020. An (arbitrary) exponential model of the pandemic evolution is  
174 superimposed to the figure (dotted red line) to describe the decreasing trend at the end of the first CoVid-  
175 19 wave; this kind of model is adopted in literature also for describing the social infection rate evolution  
176 (Duffey and Zio, 2020). The figure shows that the exponential decreases of the fatality risk due to CoVid-  
177 19 was representative of the actual evolution of pandemic for about four months. That trend suggested  
178 that the CoVid-19 risk would have been lower than the seismic one approximately at the beginning of  
179 October. However, an abrupt change in the trend of recorded fatalities occurred in the first half of August

180 and a second wave of increasing risk started, impeding the CoVid-19 risk to become lower than the seismic  
181 one.

182 It is also to note that, in Marzocchi *et al.* (2015) an upper bound threshold of the socially accepted  
183 individual risks of death (IRD) is set as 2E-06, at the weekly time scale; this value is also reported in the  
184 figure. While the seismic risk in the observed time period is always below this threshold, the CoVid-19 risk  
185 significantly exceeds the value; interesting enough is that its first exceedance is very close to the beginning  
186 of the national lockdown period while the second pandemic wave started few weeks after that the rate  
187 of deaths due to CoVid-19 reduced below the threshold. This may suggest that while the social risk  
188 perception was high and the measures to reduce the virus spreading were strictly followed, the pandemic  
189 had been actually controlled. However, as soon as the social risk perception reduced, the attention to  
190 prevent virus spreading reduced (this happened in conjunction to the period of summer vacations in Italy)  
191 and, some weeks later, the number of deaths started increasing again.

## 192 **REGIONAL SCALE**

193 The comparison between the death rates is also discussed at the regional scale because both seismic and  
194 CoVid-19 risks, for different reasons, vary within the country. First, the Abruzzo region in central Italy, is  
195 considered. Abruzzo was affected by the 2009 L'Aquila seismic sequence (Chioccarelli and Iervolino,  
196 2010). In particular, between January 2009 and June 2010, twenty-four earthquakes with magnitude equal  
197 or higher than 4.0 occurred within 50 km from the mainshock epicenter, which was the 06/04/2009  
198 Mw6.1 earthquake (Lat 42.342°, Long 13.38°) (Chioccarelli and Iervolino, 2016). In fact, one event of these  
199 preceded the mainshock and twenty-two followed it. Because of the mainshock, 308 total fatalities were  
200 counted (Dolce and Di Bucci, 2017).

201 In Figure 2 the deaths rates from OELF and those due to CoVid-19 are computed referring to the whole  
202 Abruzzo region, which is also identified in the map; the beginning and the end of the national lockdown  
203 and the IRD threshold are also reported.

204 The region is characterized by high seismicity in the Italian context; in fact, the rates from OELF are higher  
205 than those estimated at a national scale and equal to about  $1.7E-07$ . On the other hand, during the first  
206 wave, the rates of CoVid-19 deaths in this region were lower than the national ones because the region  
207 has been partially spared by the pandemic. Moreover, at the beginning of August the observed fatalities  
208 due to CoVid-19 dropped to zero so as the CoVid-19 risk represented in the figure. From August to the  
209 second half of September, the seismic risk was higher than the (observed) CoVid-19 risk. However, from  
210 the last two weeks of September to December 2020 the rates of observed deaths increased again to a  
211 maximum value equal to about  $8E-5$ .

212 In order to extend the comparison between seismic and CoVid-19 threat, a scenario analysis  
213 corresponding to the 2009 seismic sequence is also considered. Thus, in the same figure, the forecasted  
214 fatality rates (average in the whole region) computed by MANTIS-K during the seismic sequence of  
215 L'Aquila are reported (*EQ Fatality – 2009* in the figure legend), but they are associated to a different date  
216 (the main event in the figure corresponds to the 1<sup>th</sup> of June, 2020) in order to be compared with the deaths  
217 for CoVid-19 occurred in the same area in 2020. The figure shows that the considered seismic scenario  
218 caused a seismic risk comparable to the observed risk for CoVid-19 and higher than the accepted IRD.

219 Finally, in Figure 3, two other Italian regions are selected for risk comparison: Lombardia and Calabria.  
220 They are selected because representative of two opposite conditions in Italy. The former, in the norther  
221 Italy, is in the low seismic hazard area of the country (e.g., Iervolino *et al.*, 2011) and, consequently, is  
222 characterized by comparatively low seismic risk. Indeed, the expected fatalities rates from OELF on the  
223 observed period are around  $3E-08$ . However, Lombardia is one of the regions in Italy hit the hardest by  
224 the first wave of pandemic, and the maximum fatalities rates for CoVid-19 was  $3E-04$ . At the end of the

225 first wave, the new increase of pandemic risk was slower than that observed at national scale and the  
226 second peak was lower than the first. However, for the whole investigated period, the CoVid-risk is some  
227 order magnitudes larger than the seismic one. On the other hand, Calabria, in the south, is in a high seismic  
228 hazard area, comparable to central Italy, as it can be also seen by the OELF short-term results. The fatality  
229 rates from OELF are between  $1E-07$  and  $3E-07$ . This region was marginally affected by the first wave of  
230 CoVid-19 spreading: its death rates reached its maximum equal to about  $1.6E-05$  at the beginning of April  
231 and dropped to zero in the first half of June. It remained equal to zero until September when one and two  
232 fatalities were recorded in the first and the last week of the month respectively, and reached a new local  
233 maximum, larger than the first one, in December 2020.

234 In conclusion, in the northern region (low seismic hazard), the CoVid-19 related risk is several orders  
235 magnitude higher than the seismic one, whereas in the southern region (high seismic hazard) the seismic  
236 risk has been, for several weeks, comparable (or prevalent) with respect to the risk of death due to CoVid-  
237 19.

## 238 **DISCUSSION**

239 The usefulness of the OEF has been the subject of debate in the last years. Wang and Rogers (2014)  
240 claimed that the results of OEF, delivering “very low” probabilities, may be even dangerous because may  
241 suggest the idea that the society can afford to be less prepared to damaging earthquakes. However, it is  
242 shown above, that during seismic crises (e.g., the one of L’Aquila in 2009) the OELF system can provide  
243 expected values of fatalities comparable to those observed during the CoVid-19 pandemic, that has been  
244 a highly-perceived risk. Thus, using the results of OEF to perform OELF analyses allows to define measure  
245 of seismic risk that are comparable with other sources of risks.

246 Another comment of Wang and Rogers (2014) to short time variability of OEF rates is that its  
247 communication may cause panic. However, the story of the CoVid-19 pandemic demonstrates that society

248 is able to deal with significant threats with a generally correct behavior and maintaining the capacity to  
249 identify the primary necessities. More specifically, it should be noted that while during the first pandemic  
250 wave, a strict lockdown was easily accepted, during the second wave, the economic situation imposed to  
251 not completely interrupt the productive activities, despite the pandemic. Similarly, it can be assumed that,  
252 during a seismic crisis, maintaining people informed and suggesting (i.e., nudging) some behaviors, would  
253 be a practical option (see also Jordan *et al.*, 2014).

254 Referring now to the perspective of seismic risk communication, the analyzed CoVid-19 risks may be an  
255 instructive example, being the object of a worldwide attention and being sensitive to social behaviors  
256 (e.g., social distancing or lockdown) in a relatively short time window. As shown, the two waves of  
257 pandemic suggest that the correct social behavior reduces the risk, whereas, as soon as the risk becomes  
258 less perceived by the society, it may rapidly increase. This may be applied also to seismic risk that can  
259 rapidly increase as occurred during L'Aquila sequence. Although in the shown example, the increasing was  
260 due to the seismic hazard that cannot be related to the social behaviors, a reduction of the social  
261 perception of the seismic risk can reduce the social preparedness and, consequently, increase losses when  
262 earthquakes strike.

## 263 **CONCLUSIONS**

264 The comparison between the seismic and CoVid-19 risks, in term of weekly death rates, is shown at both  
265 national and regional scale. The main results that can be derived are listed in the following.

- 266 • At a national scale the CoVid-19 related risk of death has been significantly higher than the forecasted  
267 seismic risk, motivating the national priority of limiting virus' spreading. Although, for several weeks  
268 after the lockdown period, the evolution of pandemic suggested that, at the end of September, the  
269 seismic risk would have been higher than the CoVid-19 one, a new pandemic wave significantly  
270 changed the situation.

- 271 • Because of the significant variations of both seismic and CoVid-19 risks within the country, the two  
272 were also analyzed at a local (regional) scale. It was shown that among different regions, the risks  
273 comparison may provide different results. In the case of Lombardia, a low seismic and high CoVid-19  
274 risk region, the latter have always been larger than the former. On the other hand, in the opposite  
275 case of Calabria, a high seismic and low CoVid-19 risk region, the former risk was comparable to the  
276 latter for several weeks.
- 277 • Finally, in the case of Abruzzo, which is in an intermediate situation, the comparison suggests that  
278 the two risks were comparable during August and the first half of September. Moreover, for a case  
279 scenario of a seismic sequences equivalent to the deadly one occurred in 2009, the seismic risk would  
280 be comparable to the CoVid-19 fatality risk in the region observed during almost the entire period of  
281 pandemic.

282 Such results demonstrated that, although earthquakes probabilities from OEF are sometimes questioned  
283 to be negligible, their conversion in risk measures via the OELF system may provide, during seismic  
284 sequences, fatalities risks that are not negligible, being similar to those observed during the CoVid-19  
285 pandemic, an highly-perceived risk. Moreover, while the pandemic evolution may be used as a practical  
286 example of the importance of prevention and preparedness also referring to other risks, in particular to  
287 the seismic one, the social behavior, especially during the second wave, suggests that the OELF risks  
288 outcome can be communicated without inducing panic.

## 289 **DATA AND RESOURCES**

290 Data describing the evolution of the pandemic in Italy are available at the official website of the Italian  
291 government (<http://www.salute.gov.it/nuovocoronavirus>, last accessed 02/10/2020). The number of  
292 fatalities at national and regional scale are collected by the Italian Civil Protection and available at  
293 <https://github.com/pcm-dpc/COVID-19> (last accessed 22/12/2020). The characteristics of Italian

294 casualties from CoVid-19 are described at <https://www.epicentro.iss.it/en/coronavirus/sars-cov-2->  
295 [analysis-of-deaths](#). Data about population at both national and regional scale are provided by the Italian  
296 statistics institute (ISTAT) website (<http://dati.istat.it>, last accessed 02/10/2020). Operational earthquake  
297 forecasting (OEF) rates from the OEF-Italy system were provided by Prof. Warner Marzocchi. The rest of  
298 the data is from the listed references.

## 299 **ACKNOWLEDGEMENTS**

300 The work presented in this paper was developed within the H2020-SC5-2019 RISE (Real-time Earthquake  
301 Risk Reduction for a Resilient Europe) project, grant agreement 821115. The help about OEF-Italy data  
302 from prof. Warner Marzocchi (Università degli Studi di Napoli Federico II) and its comments of early draft  
303 of the manuscript are gratefully acknowledged.

## 304 **REFERENCES**

305 Chioccarelli, E., and I. Iervolino (2010). Near-source seismic demand and pulse-like records: A discussion  
306 for L'Aquila earthquake, *Earthq. Eng. Struct. Dyn.*, doi: 10.1002/eqe.987.

307 Chioccarelli, E., and I. Iervolino (2016). Operational earthquake loss forecasting: a retrospective analysis  
308 of some recent Italian seismic sequences, *Bull. Earthq. Eng.* **14**, no. 9, 2607–2626, doi:  
309 10.1007/s10518-015-9837-8.

310 Cornell, C. A., and H. Krawinkler (2000). Progress and challenges in seismic performance assessment,  
311 *PEER Cent. Newsl.* **3**, 1–3.

312 Dolce, M., and D. Di Bucci (2017). Comparing recent Italian earthquakes, *Bull. Earthq. Eng.* **15**, no. 2,  
313 497–533, doi: 10.1007/s10518-015-9773-7.

314 Duffey, R. B., and E. Zio (2020). Prediction of CoVid-19 infection, transmission and recovery rates: A new

315 analysis and global societal comparisons, *Saf. Sci.* **129**, doi: 10.1016/j.ssci.2020.104854.

316 Gorini, A., M. Nicoletti, P. Marsan, R. Bianconi, R. De Nardis, L. Filippi, S. Marcucci, F. Palma, and E.  
317 Zambonelli (2010). The Italian strong motion network, *Bull. Earthq. Eng.* **8**, no. 5, 1075–1090, doi:  
318 10.1007/s10518-009-9141-6.

319 Grünthal (ed.), G., R. Musson, J. Schwarz, and M. Stucchi (1998). European Macroseismic Scale 1998,  
320 *Cah. du Cent. Eur. Geodyn. Seismol.* **15**, 100.

321 Gutenberg, B., and C. F. Richter (1944). Frequency of earthquakes in California, *Bull. Seismol. Soc. Am.*  
322 **34**, 185–188.

323 Iervolino, I., E. Chioccarelli, and V. Convertito (2011). Engineering design earthquakes from multimodal  
324 hazard disaggregation, *Soil Dyn. Earthq. Eng.* **31**, no. 9, 1212–1231, doi:  
325 10.1016/j.soildyn.2011.05.001.

326 Iervolino, I., E. Chioccarelli, M. Giorgio, W. Marzocchi, G. Zuccaro, M. Dolce, and G. Manfredi (2015).  
327 Operational (short-term) earthquake loss forecasting in Italy, *Bull. Seismol. Soc. Am.* **105**, no. 4,  
328 2286–2298, doi: 10.1785/0120140344.

329 Iervolino, I., E. Chioccarelli, and A. Suzuki (2020). Seismic damage accumulation in multiple mainshock –  
330 aftershock sequences, *Earthq. Eng. Struct. Dyn.* **49**, no. 10, 1007–1027, doi: 10.1002/eqe.3275.

331 Jordan, T. H., W. Marzocchi, A. J. Michael, and M. C. Gerstenberger (2014). Operational earthquake  
332 forecasting can enhance earthquake preparedness, *Seismol. Res. Lett.* **85**, no. 5, 955–959, doi:  
333 10.1785/0220140143.

334 Margheriti, L., M. Quintilian, A. Bono, V. Lauciani, F. Bernardi, C. Nostro, M. C. Lorenzino, S. Pintore, F.  
335 M. Mele, E. Ruotolo, *et al.* (2021). #IStayhome and Guarantee Seismic Surveillance and Tsunami  
336 Warning during the COVID-19 Emergency in Italy, *Seismol. Res. Lett.* **92**, no. 1, 53–59.



337 Marzocchi, W., I. Iervolino, M. Giorgio, and G. Falcone (2015). When Is the Probability of a Large  
338 Earthquake Too Small?, *Seismol. Res. Lett.* **86**, no. 6, 1674–1678, doi: 10.1785/0220150129.

339 Marzocchi, W., A. M. Lombardi, and E. Casarotti (2014). The Establishment of an Operational Earthquake  
340 Forecasting System in Italy, *Seismol. Res. Lett.* **85**, no. 5, 961–969, doi: 10.1785/0220130219.

341 Pankow, K. L., J. Rusho, J. C. Pechmann, J. M. Hale, K. Whidden, R. Sumsion, J. Holt, M. Mesimeri, D.  
342 Wells, and K. D. Koper (2020). Responding to the 2020 Magna, Utah, Earthquake Sequence during  
343 the COVID-19 Pandemic Shutdown, *Seismol. Res. Lett.* **92**, no. 1, doi: 10.1785/0220200265.

344 Pasolini, C., P. Gasperini, D. Albarello, B. Lolli, and V. D’Amico (2008). The attenuation of seismic  
345 intensity in Italy, Part I: Theoretical and empirical backgrounds, *Bull. Seismol. Soc. Am.* **98**, no. 2,  
346 682–691, doi: 10.1785/0120070020.

347 Peng, Z. (2020). Earthquakes and Coronavirus: How to Survive an Infodemic, *Seismol. Res. Lett.*, doi:  
348 10.1785/0220200125.

349 Sieberg, A. (1931). Erdebeben, in *Handbuch der Geophysik*, **4**, 552–554.

350 Wang, K., and G. C. Rogers (2014). Earthquake preparedness should not fluctuate on a daily or weekly  
351 basis, *Seismol. Res. Lett.* **85**, no. 3, 569–571, doi: 10.1785/0220130195.

352 Woessner, J., J. Woessner, A. Christophersen, J. D. Zechar, and D. Monelli (2010). Building self-  
353 consistent, short-term earthquake probability (STEP) models: improved strategies and calibration  
354 procedures, *Ann. Geophys.* **53**, no. 3, 141–154, doi: 10.4401/ag-4812.

355 Zuccaro, G., and F. Cacace (2009). Revisione dell’inventario a scala nazionale delle classi tipologiche di  
356 vulnerabilità ed aggiornamento delle mappe nazionali di rischio sismico, in *XIII Convegno*  
357 *l’Ingegneria Sismica in Italia, ANIDIS, Bologna, Italy, N. S4.39.*

358 Zuccaro, G., and F. Cacace (2011). Seismic casualty evaluation: the Italian model, an application to the  
359 L'Aquila 2009 event, *Hum. Casualties Earthquakes Prog. Model. Mitig.*, 171–184.

360 Zuccaro, G., F. Cacace, and D. De Gregorio (2012). Buildings inventory for seismic vulnerability  
361 assessment on the basis of Census data at national and regional scale, in *15th World Conference on*  
362 *Earthquake Engineering*.

### 363 **FIGURE CAPTIONS**

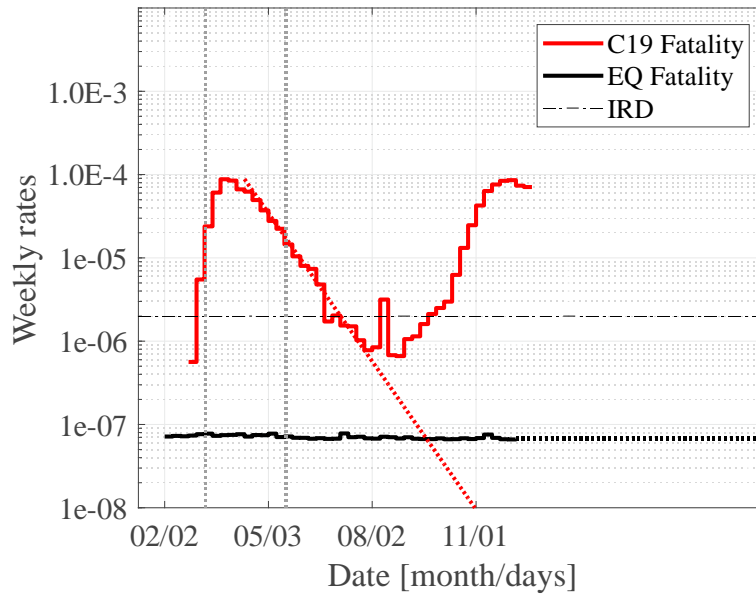
364 **Figure 1. Comparisons of risks measures at the national scale in 2020: weekly rates of (i) expected fatalities due to earthquakes,**  
365 **(ii) observed fatalities due to CoVid-19 infection. The red dotted line provides the expected intersection of CoVid-19 and**  
366 **seismic risk after the first wave.**

367 **Figure 2. Comparisons of risks measures for the Abruzzo region (identified in the map) in 2020: weekly rates of (i) expected**  
368 **fatalities due to earthquakes, (ii) observed fatalities due to CoVid-19 infection, (iii) expected fatalities estimated during the**  
369 **seismic sequence of 2009.**

370 **Figure 3. Comparisons of risks measures for the Lombardia and Calabria regions (colored grey and blue in the map, respectively)**  
371 **in 2020: weekly rates of (i) expected fatalities due to earthquakes, (ii) observed fatalities due to CoVid-19 infection.**

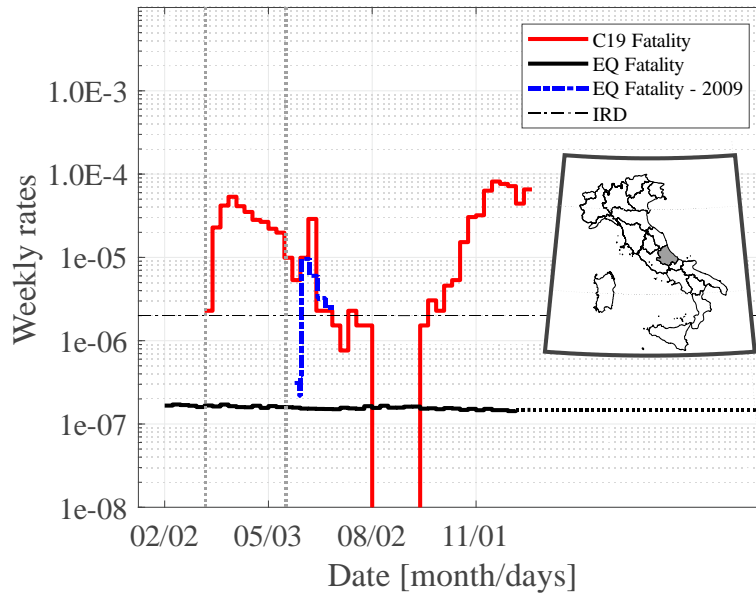
372

373 **FIGURES**



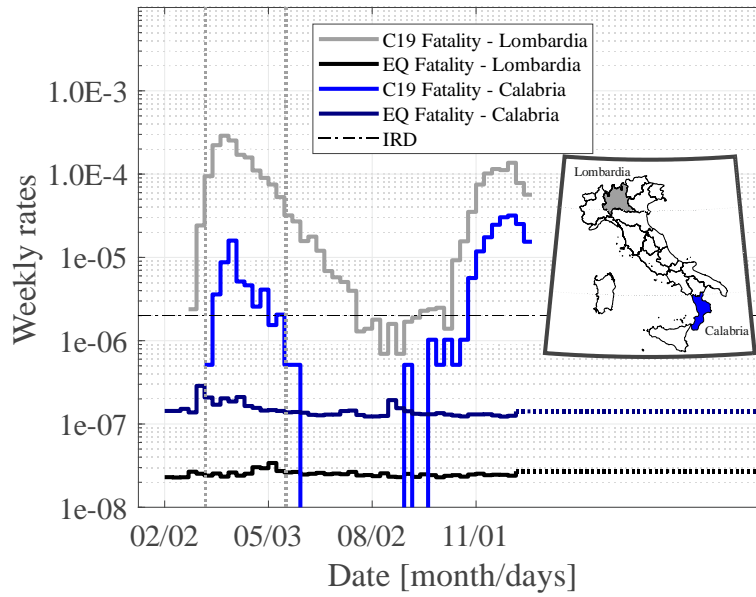
374

375 **Figure 1. Comparisons of risks measures at the national scale in 2020: weekly rates of (i) expected fatalities due to earthquakes,**  
376 **(ii) observed fatalities due to CoVid-19 infection. The red dotted line provides the expected intersection of CoVid-19 and**  
377 **seismic risk after the first wave.**



378

379 **Figure 2. Comparisons of risks measures for the Abruzzo region (identified in the map) in 2020: weekly rates of (i) expected**  
 380 **fatalities due to earthquakes, (ii) observed fatalities due to CoVid-19 infection, (iii) expected fatalities estimated during the**  
 381 **seismic sequence of 2009.**



382

383 **Figure 3. Comparisons of risks measures for the Lombardia and Calabria regions (colored grey and blue in the map, respectively)**

384 **in 2020: weekly rates of (i) expected fatalities due to earthquakes, (ii) observed fatalities due to CoVid-19 infection.**